EXPERIMENTAL POINCARE MAPS FROM THE TWIST-AND-FLIP CIRCUIT

by

Guo-Qun Zhong, Leon O. Chua, and Ray Brown

Memorandum No. UCB/ERL M95/110

1 October 1995

COVER PAGE

EXPERIMENTAL POINCARE MAPS FROM THE TWIST-AND-FLIP CIRCUIT

by

Guo-Qun Zhong, Leon O. Chua, and Ray Brown

Memorandum No. UCB/ERL M95/110

1 October 1995

ELECTRONICS RESEARCH LABORATORY

College of Engineering
University of California, Berkeley
94720

Experimental Poincaré Maps from the Twist-and-Flip Circuit

Guo-Qun Zhong*, Leon O. Chua, and Ray Brown

Abstract

In this paper, we present a physical implementation of the twist-and-flip circuit containing a nonlinear gyrator. Many *phase portraits* and their associated *Poincaré maps* are observed experimentally from this circuit and presented in this paper.

1. Introduction

Fractals are one of many manifestations of complicated chaotic dynamics. The fractal phenomenon can occur not only in autonomous systems typical of Chua's circuit [1]–[3], but also in nonautonomous systems driven by time-varying signals and therefore described by a nonautonomous system of ordinary differential equations

$$\dot{\mathbf{x}} = f(\mathbf{x}, t) \tag{1}$$

where $\mathbf{x}$ is a vector in an n-dimensional Euclidean space $\mathbf{R}^n$.

The twist-and-flip circuit offers one of the simplest paradigms for nonautonomous chaos. Indeed, the state equations associated with the twist-and-flip circuit are the only known nonautonomous system of ordinary differential equations whose Poincaré map can be derived in an *explicit analytic* form. Based on this property of the circuit an in-depth mathematical analysis of the twist-and-flip map has been carried out exhaustively and rigorously [4]–[5]. The various fractals corresponding to several classes of nonlinear gyration conductance functions $g(v_1, v_2)$ from this map have been generated numerically [6].

In this paper we describe a physical implementation of the *twist-and-flip circuit* with a simple nonlinear gyration conductance function $g(v_1, v_2)$, driven by a square-wave voltage source. A variety of phase portraits and the corresponding Poincaré maps observed experimentally from this setup will be presented.

2. Physical implementation of the twist-and-flip circuit

The twist-and-flip circuit contains simply two linear capacitors C_1 and C_2, a voltage source $s(t)$, and a *nonlinear* gyrator, as shown in Fig. 1(a). The voltage source $s(t)$ for driving the circuit is a square wave of amplitude a and angular frequency ω (or period $P = \frac{2\pi}{\omega}$), as shown in Fig. 1(b). The gyrator, which is the only nonlinear element in the circuit, is described by the equations

*He is on leave from Guangzhou Institute of Electronic Technology, Academia Sinica, Guangzhou 510070, People's Republic of China.

$$\left.\begin{aligned} i_1 &= g(v_1, v_2)v_2 \\ i_2 &= -g(v_1, v_2)v_1 \end{aligned}\right\} \tag{2}$$

where $g(v_1, v_2)$ is the associated gyration conductance [7]. In this paper we assume that

$$g(v_1, v_2) > 0, \text{ for } -\infty < v_1, v_2 < \infty.$$

2.1 State equations of the twist-and-flip circuit

Applying **KCL** and **KVL** to the circuit shown in Fig. 1(a), we obtain

$$\left.\begin{aligned} i_1 &= -C_1\tfrac{dx}{dt} \\ i_2 &= -C_2\tfrac{dy}{dt} \end{aligned}\right\} \tag{3}$$

where

$$\begin{aligned} v_1(t) &= x(t) - s(t), \\ v_2(t) &= y(t). \end{aligned}$$

Introducing equations (2) into equations (3) and normalizing $C_1 = C_2 = 1$, we obtain the following state equations governing the dynamics of the twist-and-flip circuit:

$$\tfrac{dx}{dt} = -g\left(x - s(t), y\right) y \tag{4a}$$

$$\tfrac{dy}{dt} = g\left(x - s(t), y\right)\left(x - s(t)\right) \tag{4b}$$

where

$$\begin{aligned} s(t) = a, \quad & t \in (n, n+\tfrac{1}{2})P \text{ (positive-half cycle)} \\ s(t) = -a, \quad & t \in (n+\tfrac{1}{2}, n+1)P \text{ (negative-half cycle)} \\ & n = 0, 1, 2, \cdots. \end{aligned}$$

Dividing (4b) by (4a), we obtain

$$\tfrac{dy}{dx} = -\tfrac{(x-a)}{y} \tag{5a}$$

and

$$\tfrac{dy}{dx} = -\tfrac{(x+a)}{y} \tag{5b}$$

over each positive- and negative-half cycles, respectively. Obviously, equation (5) defines a phase portrait consisting of a family of concentric circles, centered at $x = a$ over each positive-half cycle $t \in (n, n+\frac{1}{2})P$, and at $x = -a$ over each negative-half cycle $t \in (n+\frac{1}{2}, n+1)P, n = 0, 1, 2, \cdots$, as shown in Figs. 2(a)–(b) . The phase portrait over a full period is shown in Fig. 2(c).

2.2 Implementation of the twist-and-flip circuit

To implement the twist-and-flip circuit shown in Fig. 1(a), we must specify the nonlinear gyration conductance function $g(v_1, v_2)$ for the circuit. In this paper we choose

$$g(v_1, v_2) = \sqrt{v_1^2 + v_2^2}. \tag{6}$$

The block diagram of the physical implementation for the twist-and-flip circuit is shown in Fig. 3(a). It consists of two squaring functional blocks, two multipliers, two voltage-controlled current sources, one adder, one square-root functional block, two linear capacitors C_1 and C_2, and a square-wave voltage source $s(t)$. The two squaring functional blocks, the adder, and the square-root functional block together perform the task to realize the gyration conductance function (6). The two analog multipliers and voltage-controlled current sources together realize the equation (2). The capacitors C_1 and C_2 are connected across port 1 and port 2 of the gyrator, respectively. The input signal to the twist-and-flip circuit is $s(t)$, a square-wave voltage source with amplitude a and angular frequency ω. The analog multipliers AD633JN and AD734AN are respectively used to implement all multiplications, squaring, and square-rooting operations in Fig. 3(a). The complete circuit diagram of the twist-and-flip circuit is shown in Fig. 3(b).

3. Experimental observations of Poincaré maps in the twist-and-flip circuit

Though the twist-and-flip circuit has an explicit mathematical solution, its asymptotic behavior in the $x - y$ phase plane is nevertheless muddled by an infinite tangle of intersections of the trajectory upon itself. The standard method to untangle such a mess of points and extract some useful asymptotic information is to analyze the dynamics of the associated Poincaré map defined as follows: Given any point (x_0, y_0), the Poincaré map of (x_0, y_0) for the circuit is a point (x_1, y_1) that corresponds to the position of the trajectory (originating from (x_0, y_0)) at $t = P = \frac{2\pi}{\omega}$ [6].

Fig. 4 shows the circuit setup used in our experimental observations of the Poincaré map. The sampled-and-hold output signals x and y of the circuit are connected respectively to the horizontal and vertical channels of an oscilloscope, operating in X-Y mode. The sample-and-hold impulse is generated by the square-wave voltage source $s(t)$ used for driving the twist-and-flip circuit.

By changing the amplitude a or the period P of the square-wave voltage source $s(t)$, a rich variety of phase portraits, including chaotic and periodic behaviors, have been observed from the implemented twist-and-flip circuit. The experimentally constructed phase portrait, and its corresponding Poincaré map in the $x - y$ plane, are shown in Figs. 5(a)–(f). Note that the phase portrait in the $x - y$ plane is muddled by an infinite tangle of intersections of the trajectory upon itself, whereas the corresponding Poincaré map in the $x - y$ plane is a clearly defined set of points illustrating the chaotic attractor occurring in the twist-and-flip circuit. To compare with theoretic results, the Poincaré maps obtained by numerical simulation for the circuit operating in a chaotic regime are shown in Figs. 6(a)–(f). The simulation is based on Eqs. (4a) and (4b), in which capacitances C_1 and C_2 are normalized to 1. The twist-and-flip circuit is theoretically lossless. However, the physical realization of this circuit must necessarily involve some losses, however small. These losses, or damping factors are nonlinear and very difficult to model exactly. Therefore, to construct a reasonable simulation requires some approximations to these losses. The way to include damping in the twist-and-flip mapping is suggested by the dissipative example in [4], and the derivations of dissipative Poincaré maps in [5]. Using these results we include two dissipative parameters in the simulations, α, and β. The resulting simulations of the Poincaré maps shown in Figs. 6(a)–(f) have the same voltages and frequencies utilized in the circuit corresponding to Figs. 5(a)–(f). While the correspondences are not exact, the differences we believe are due to the difficulties of capturing the exact form of the nonlinear dissipative terms to be included in the twist-and-flip maps used to simulate the circuit. Given this qualification, several of the Poincaré maps occurring in Fig. 5 are in excellent geometric agreement to what is seen in typical dissipative twist-and-flip maps. From

this we conclude that this circuit is a good electronic realization of the twist-and-flip paradigm of chaos.

The trajectory is stable when the circuit operates in a periodic regime. In this case, the phase portrait in the $x - y$ plane is stationary, and the Poincaré map is a set of periodic points. When a square wave of amplitude $a = 0$ over each negative-half cycle is used as the sample-and-hold voltage, we obtain the display shown in Figs. 7(a)–(b), in which the phase portrait and its Poincaré map over each positive-half cycle of the square-wave voltage source $s(t)$ appear simultaneously.

4. Concluding remarks

The most remarkable property of the twist-and-flip circuit is that its associated nonautonomous state equations have an *explicit* and *simple* Poincaré map, making it mathematically tractable. This circuit is imbued with a full repertoire of complicated chaotic dynamics. In this paper , we have implemented the twist-and-flip circuit having a nonlinear *gyration conductance function* defined by $g(v_1, v_2) = \sqrt{v_1^2 + v_2^2}$, and presented simulated numerically observations utilizing the twist-and-flip map model with losses. Due to the complex nature of the actual model for the losses and the sensitivity of the dissipative Poincaré map to the nonlinear dissipative parameters, constructing the exact damping model is difficult and is an open question for further study. Utilizing the same circuit synthesis technique, a rich variety of Poincaré maps can be observed experimentally by synthesizing other twist-and-flip circuits having more complicated gyration conductance functions, such as those presented in [6].

Acknowledgment

This work was supported in part by the Office of Naval Research under Grant N00014-89-J-1402 and by the National Science Foundation under Grant MIP 86-14000.

One of the authors, G. Q. Zhong, would like to thank C. W. Wu for helpful discussions.

References

[1] L. O. Chua, "The genesis of Chua's circuit," *Archiv Elektronik Ubertragungstechnik,* vol. 46, no. 4, pp. 250–257, 1992.

[2] R. N. Madan, Guest Ed., Special Issue on "Chua's Circuit: A Paradigm for Chaos", *J. Circuits, Syst. Computers,* Part I: Mar. 1993; Part II: June 1993.

[3] G. Q. Zhong and F. Ayrom, "Experimental confirmation of chaos from Chua's circuit," *Int. J. Circuit Theory Appl.* vol. 13, no.1, pp. 93–98, 1985.

[4] R. Brown and L. O. Chua, "Horseshoes in the twist-and-flip map," *Int. J. Bifurcation Chaos,* vol. 1, no. 1, pp. 235–252, 1991.

[5] R. Brown and L. O. Chua, "Generalizing the twist-and-flip paradigm ," *Int. J. Bifurcation Chaos,* vol. 1, no. 2, pp. 385–416, 1991.

[6] L. O. Chua, R. Brown, and N. Hamilton, "Fractals in the twist-and-flip circuit," *Proc. of IEEE,* vol. 81, no. 10, pp. 1466–1491, Oct. 1993.

[7] L. O. Chua, *Introduction to Nonlinear Network Theory.* McGraw-Hill, 1969.

Figure Captions

Fig. 1 (a) Twist-and-flip circuit containing two linear capacitors and a gyrator characterized by a nonlinear gyration conductance function $g(v_1, v_2)$, driven by a voltage source $s(t)$.
(b) Voltage source $s(t)$ in (a), a square wave with amplitude a and angular frequency ω.

Fig. 2 (a) Phase portrait centered at $x = a$ over each positive-half cycle of $s(t)$.
(b) Phase portrait centered at $x = -a$ over each negative-half cycle of $s(t)$.
(c) Combined phase portrait over a full period of $s(t)$.

Fig. 3 (a) Block diagram of physical implementation for the twist-and-flip circuit.
(b) Implemented circuit diagram of the twist-and-flip circuit.

Fig. 4 Experimental setup for observing the Poincaré map.

Fig. 5 Experimentally observed phase portrait (left) and its corresponding Poincaré map (right) of the twist-and-flip circuit, driven by a square-wave voltage source $s(t)$ with the circuit operating in a chaotic regime. Horizontal axis is x, vertical axis is y. Parameter values: (a) $a = 1.0V, P = 1.8ms$; (b) $a = 1.5V, P = 2.4ms$; (c) $a = 2.0V, P = 1.35ms$; (d) $a = 2.0V, P = 1.7ms$; (e) $a = 2.5V, P = 1.3ms$; (f) $a = 3.0V, P = 0.81ms$.

Fig. 6 Numerically simulated Poincaré map for the circuit operating in a chaotic regime. Horizontal axis is x, vertical axis is y. Parameter values: (a) $a = 1.0V, P = 1.8ms, \alpha = 0.013, \beta = 3$; (b) $a = 1.5V, P = 2.4ms, \alpha = 0.026, \beta = 2.3$; (c) $a = 2.0V, P = 1.35ms, \alpha = 0.02, \beta = 1.5$; (d) $a = 2.0V, P = 1.7ms, \alpha = 0.02, \beta = 2.5$; (e) $a = 2.5V, P = 1.3ms, \alpha = 0.020605, \beta = 2.2686$. (f) $a = 3.0V, P = 0.81ms, \alpha = 0.006, \beta = 5.8$.

Fig. 7 Phase portrait and Poincaré map experimentally observed with the circuit operating in a chaotic regime. Horizontal axis is x, vertical axis is y. $a = 3.0V, P = 2.4ms$.
(a) Phase portrait in $x-y$ plane; (b) Corresponding Poincaré map superimposed on the phase portrait over each positive-half cycle of $s(t)$.

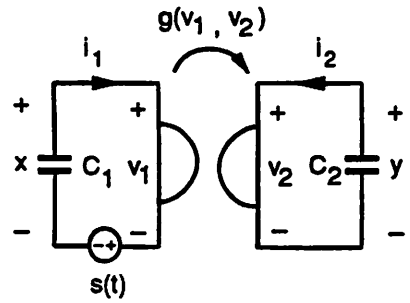

(a)

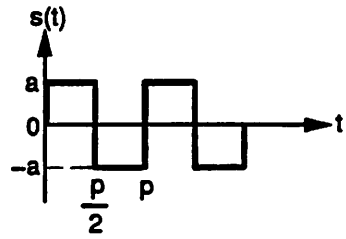

(b)

Fig. 1

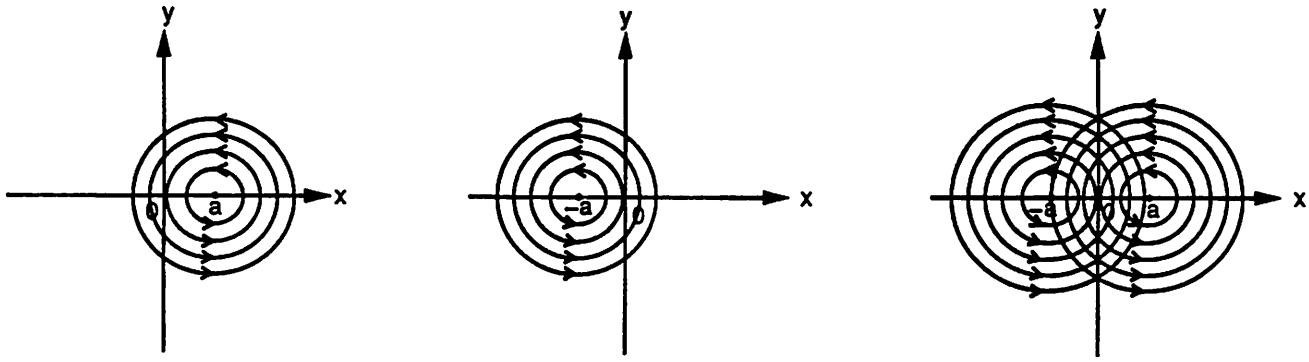

(a) (b) (c)

Fig. 2

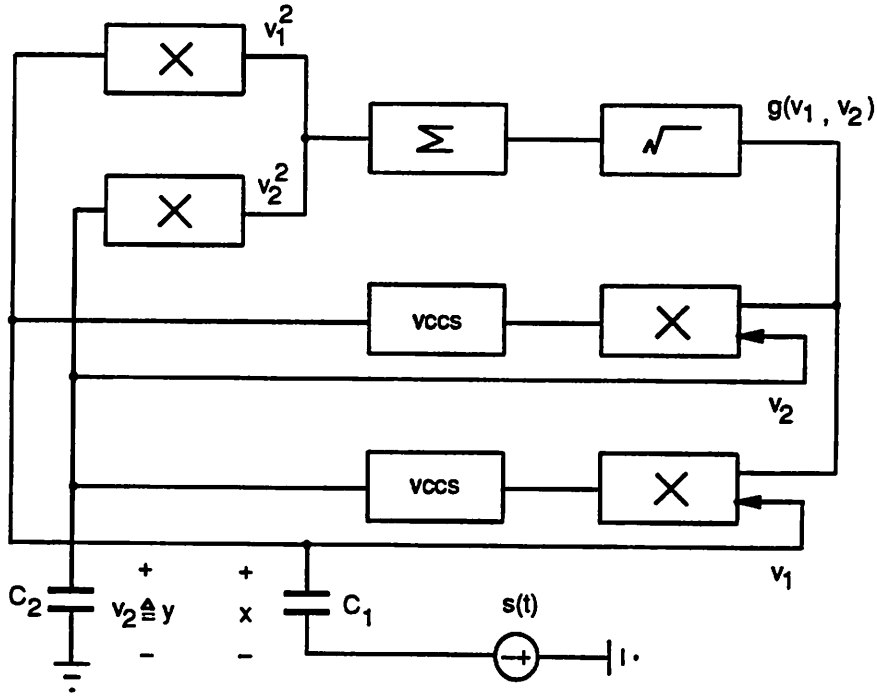

Fig. 3 (a)

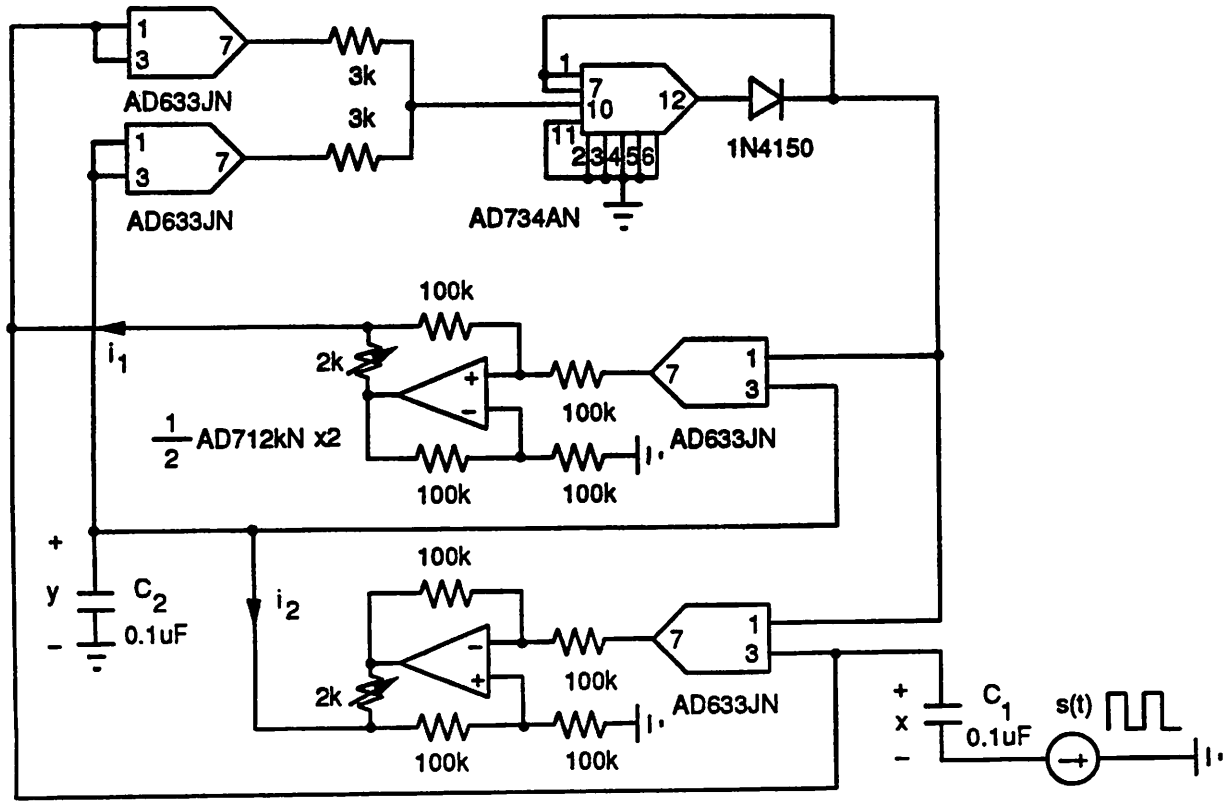
AD633JN
3k
3k
AD633JN
AD734AN
1N4150
100k
i_1
2k
100k
$\frac{1}{2}$ AD712kN x2
AD633JN
100k
100k
y
C_2
0.1uF
i_2
100k
2k
100k
AD633JN
100k
100k
x
C_1
0.1uF
s(t)

Fig. 3(b)

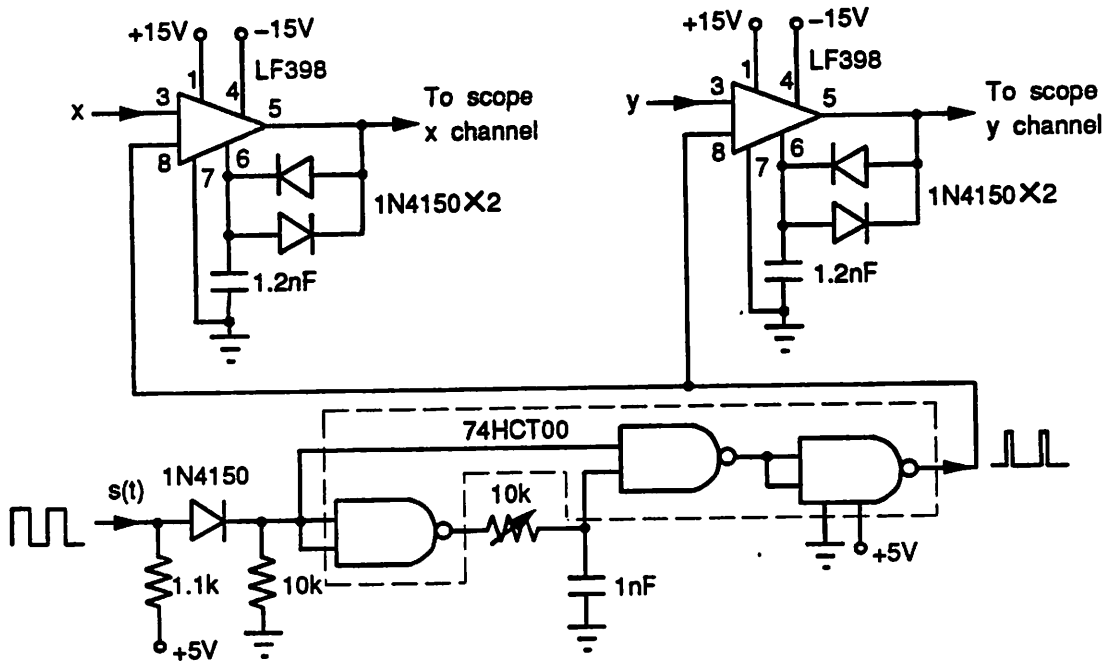
+15V
-15V
LF398
x
To scope
x channel
1N4150X2
1.2nF
+15V
-15V
LF398
y
To scope
y channel
1N4150X2
1.2nF
74HCT00
s(t)
1N4150
10k
1.1k
10k
1nF
+5V
+5V

Fig. 4

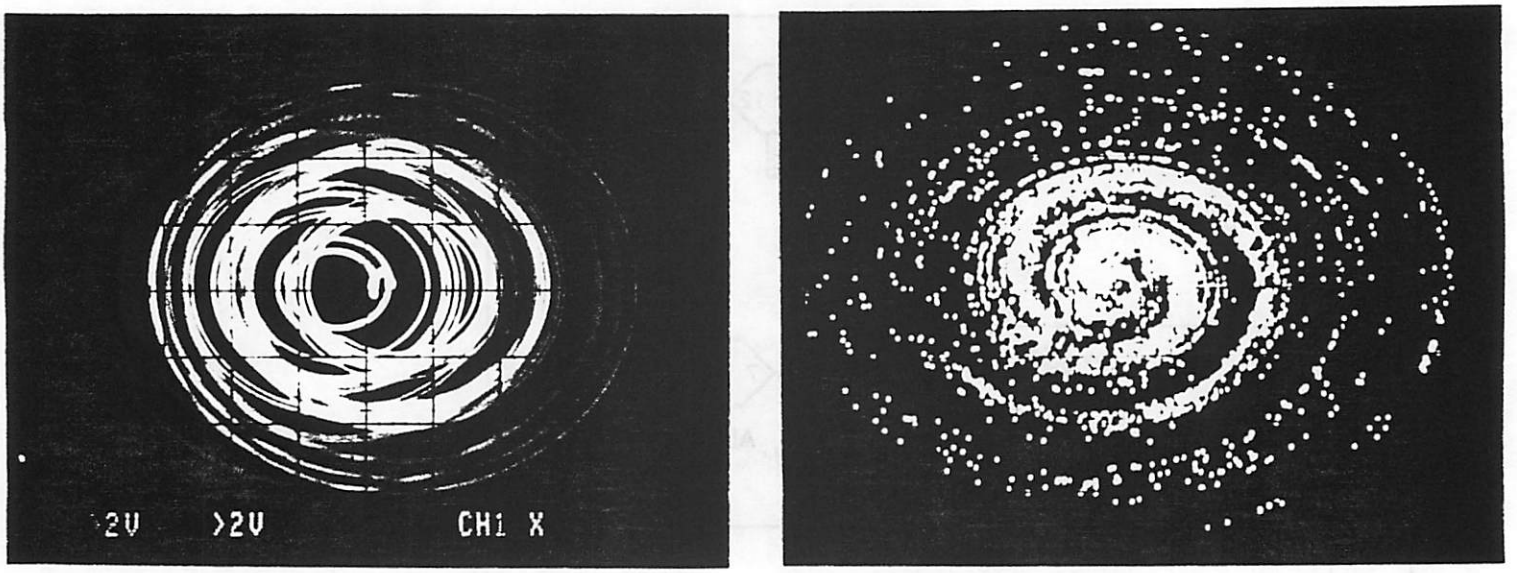

(a)

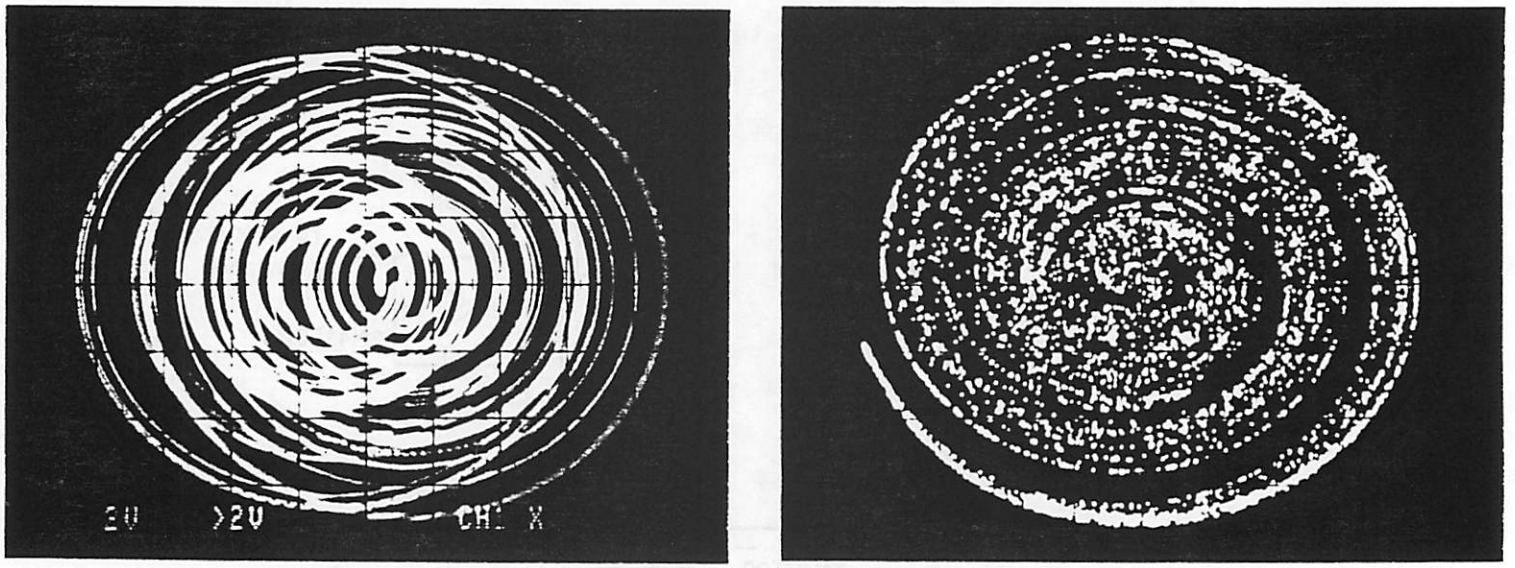

(b)

Fig. 5

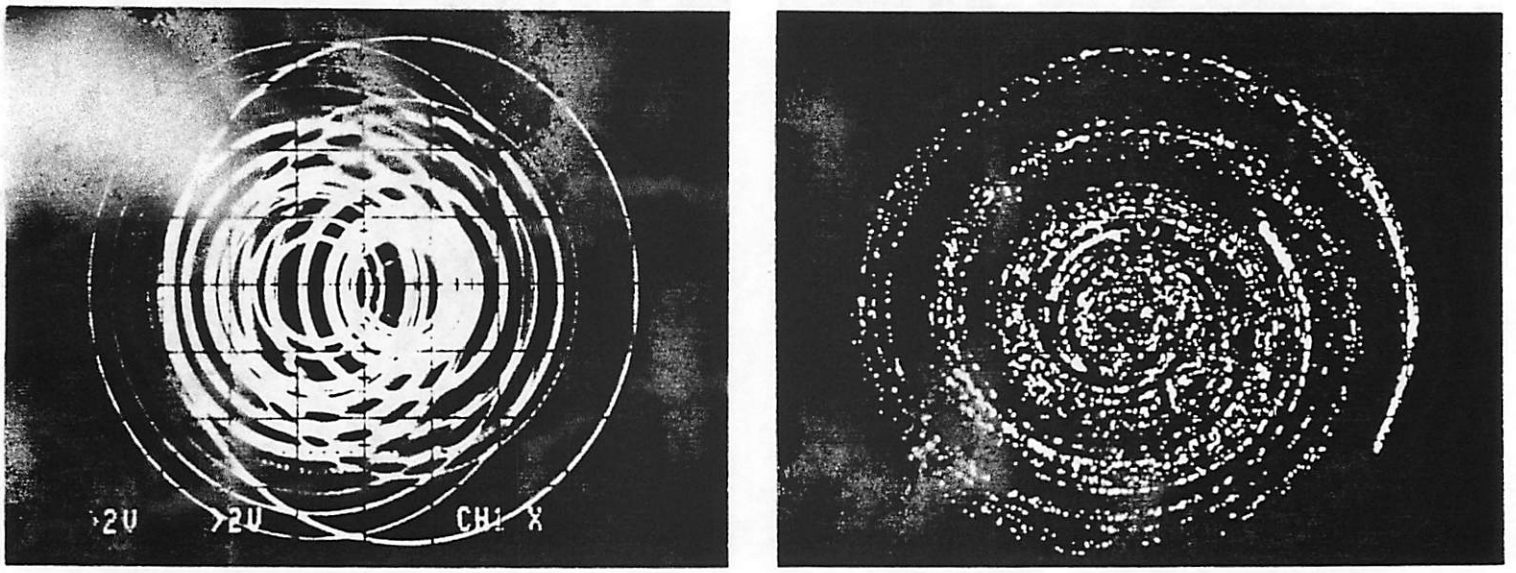

(c)

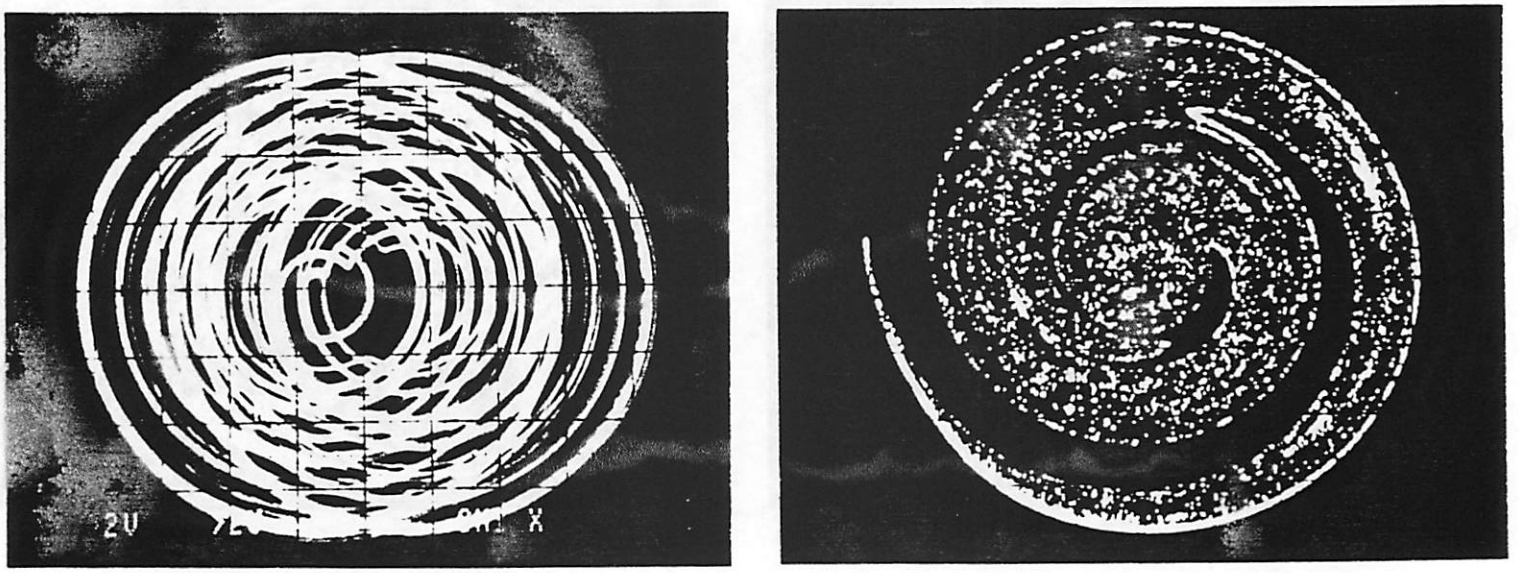

(d)

Fig. 5

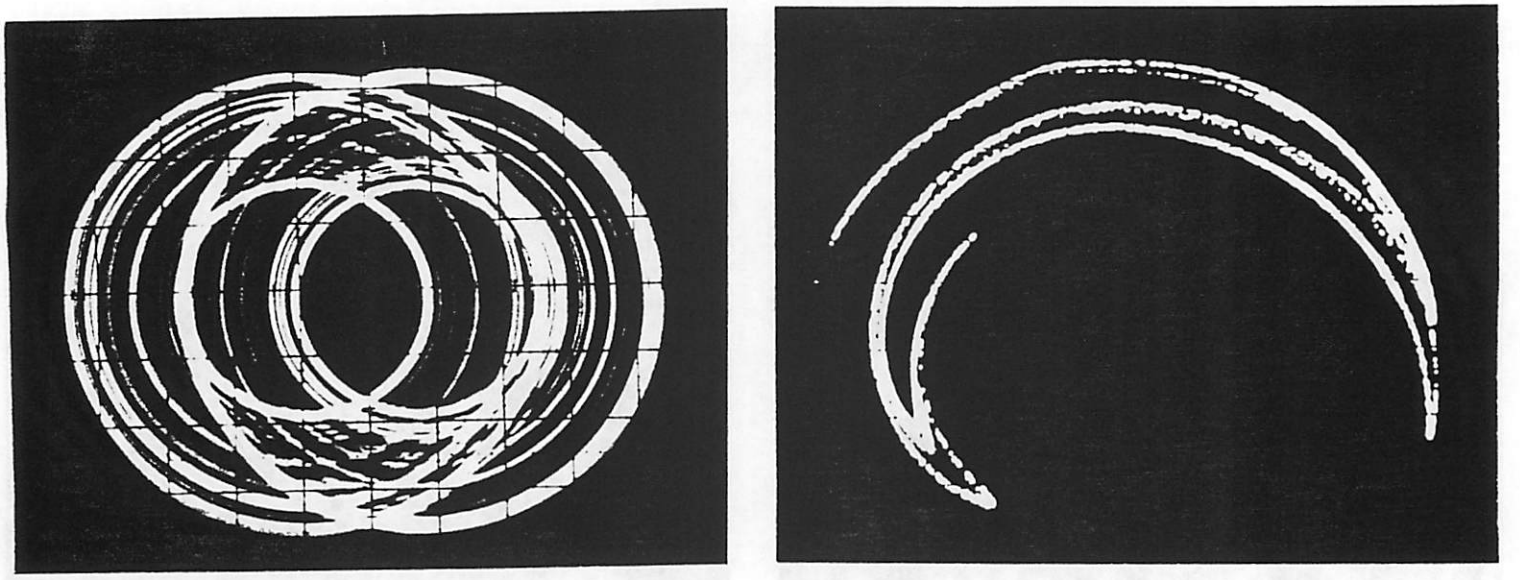

(e)

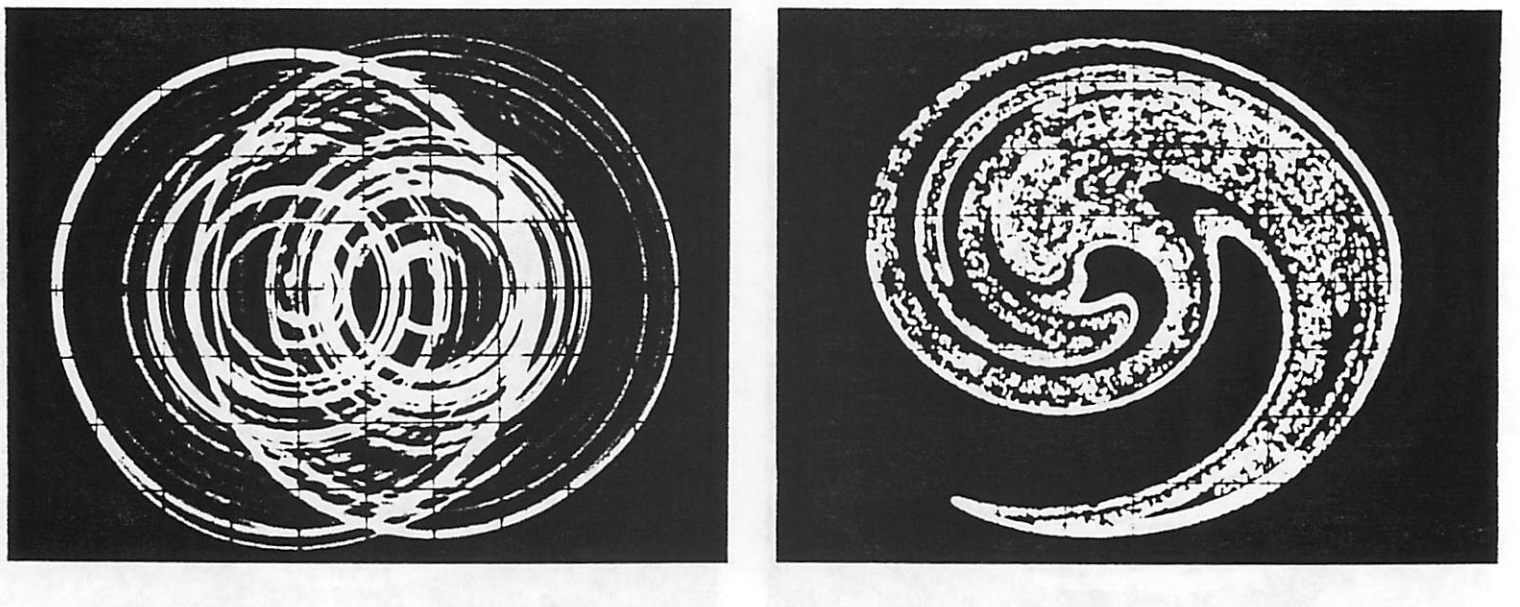

(f)

Fig. 5

(a)

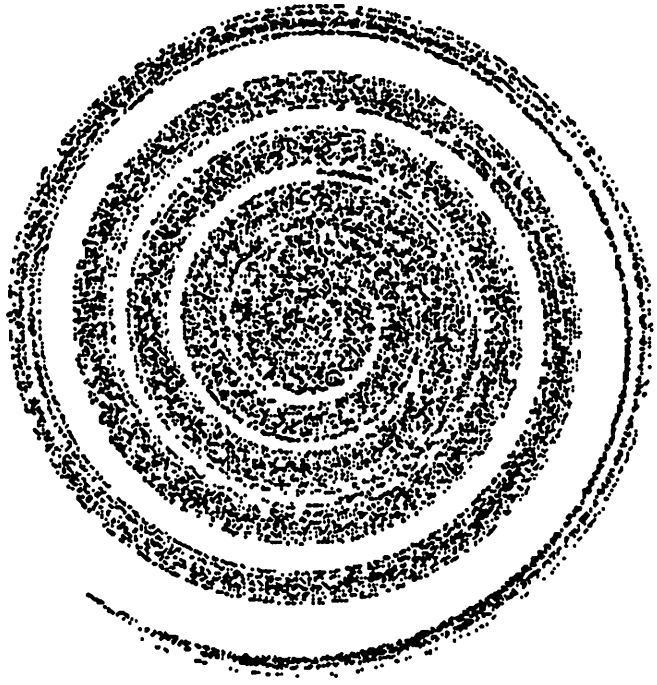

(b)

Fig. 6

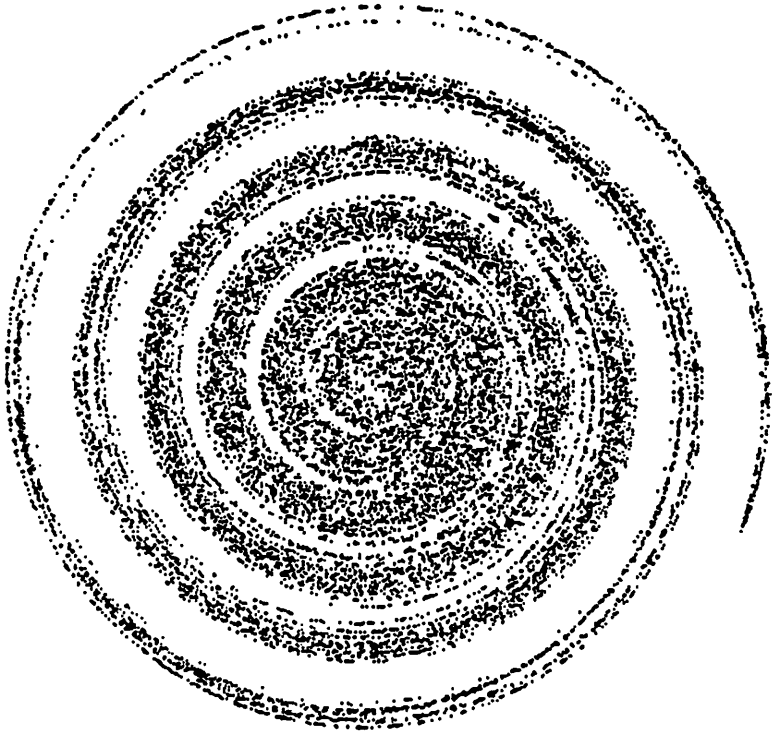

(c)

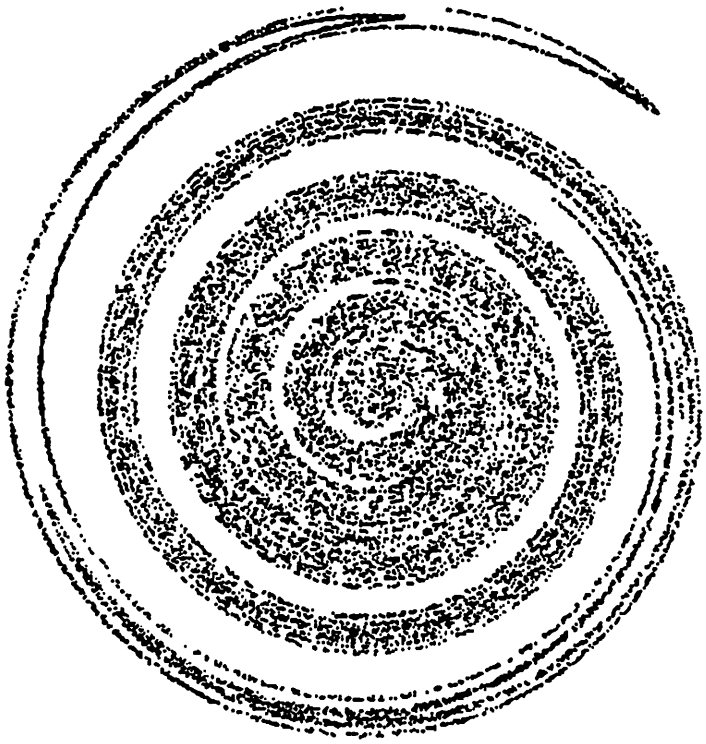

(d)

Fig. 6

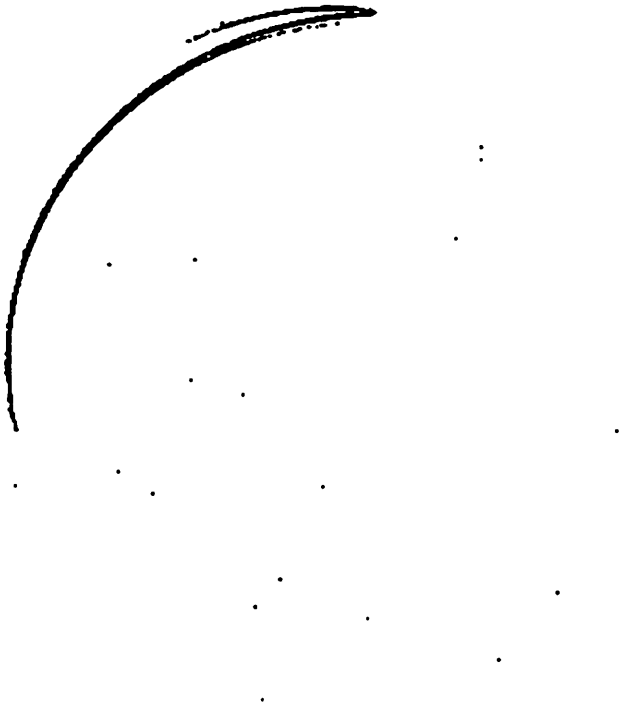

(e)

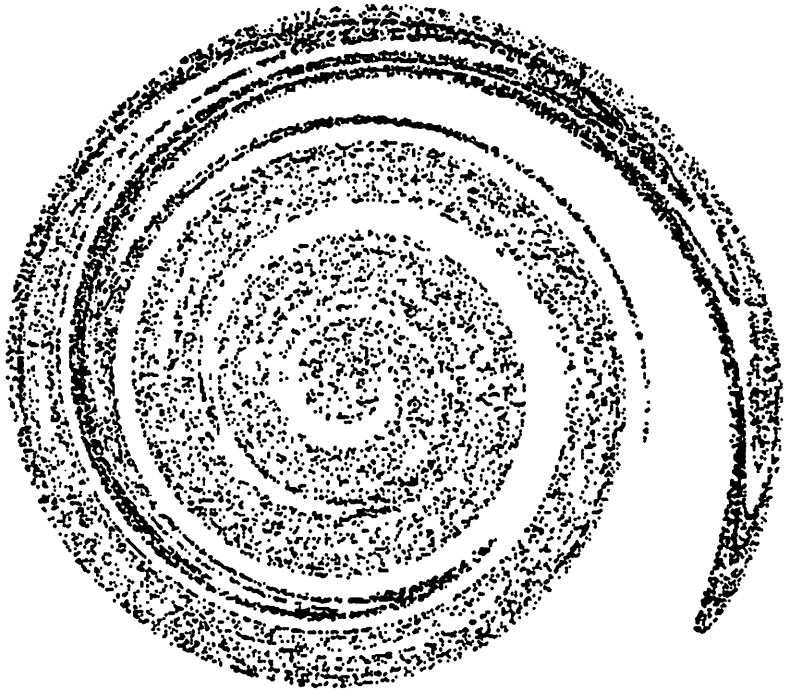

(f)

Fig. 6

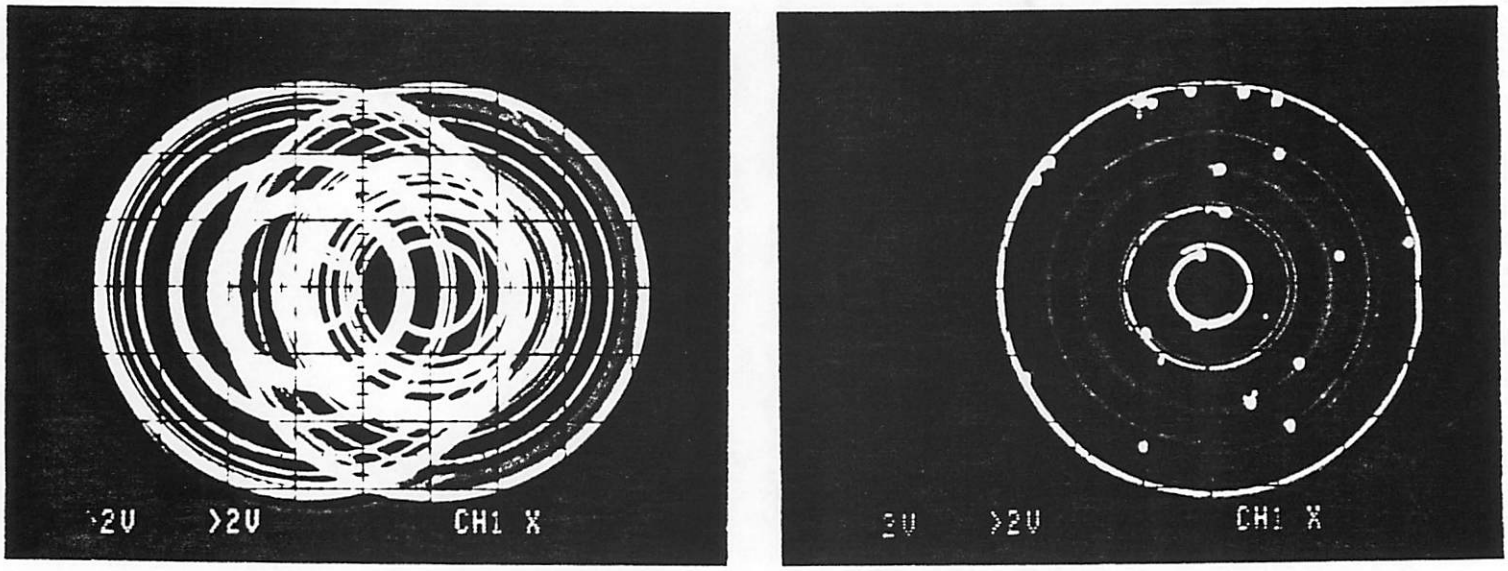

(a) (b)

Fig. 7